The Carbon Tetrachloride (CCl_4) Budget: Mystery or Not

Qing Liang[1,2], Paul A. Newman[1], John S. Daniel[3], Stefan Reimann[4], Bradley Hall[5], Geoff Dutton[5,6], Lambert J. M. Kuijpers[7]

[1] NASA Goddard Space Flight Center, Atmospheric Chemistry and Dynamics Laboratory, Greenbelt, MD 20771, USA.

[2] Universities Space Research Association, GESTAR, Columbia, MD 21044, USA.

[3] National Oceanic and Atmospheric Administration, Earth System Research Laboratory, Chemical Sciences Division, 325 Broadway, Boulder, CO 80305, USA.

[4] Empa, Swiss Federal Laboratories for Materials Science and Technology, Dübendorf, Switzerland.

[5] National Oceanic and Atmospheric Administration, Earth System Research Laboratory, Global Monitoring Division, 325 Broadway, Boulder, CO 80305, USA.

[6] Cooperative Institute for Research in Environmental Sciences, University of Colorado at Boulder, Boulder, CO 80309, USA.

[7] Technical University Eindhoven, Eindhoven, Netherlands.

Key Points

- Interhemispheric gradient can serve as a proxy to constrain CCl_4 emissions.
- A minimum 30 Gg/yr CCl_4 emissions is necessary to reconcile the observations.
- The likely lifetime for CCl_4 is 25-36 years, longer than the current estimate.

Keywords

Carbon Tetrachloride budget; CCl_4; interhemispheric gradient; lifetime; emission

Abstract

Carbon tetrachloride (CCl_4) is a major anthropogenic ozone-depleting substance and greenhouse gas and has been regulated under the Montreal Protocol. However, atmospheric observations show a very slow decline in CCl_4 concentrations, inconsistent with the nearly zero emissions estimate based on the UNEP reported production and feedstock usage in recent years. It is now apparent that there are either unidentified industrial leakages, an unknown production source of CCl_4, or large legacy emissions from CCl_4 contaminated sites. In this paper we use a global chemistry climate model to assess the budget mystery of atmospheric CCl_4. We explore various factors that affect the global trend and the gradient between the Northern and Southern hemispheres or interhemispheric gradient (IHG): emissions, emission hemispheric partitioning, and lifetime variations. We find a present-day emission of 30-50 Gg/yr and a total lifetime ~25-36 years are necessary to reconcile both the observed CCl_4 global trend and IHG.

Index terms

Constituent sources and sinks; Troposphere: constituent transport and chemistry; Air/sea constituent fluxes.

1. Introduction

Carbon tetrachloride (CCl_4) is primarily used as a feedstock or processing agent for chlorinated species, but has been used extensively as a cleaning agent and as a solvent in the past [*CTOC Report, UNEP*, 2011]. CCl_4 is recognized as both an ozone-depleting substance (ODS) and a greenhouse gas. As of 2008, CCl_4 accounted for about 11% of total tropospheric chlorine [*WMO*, 2011]. The ozone depletion potential (with respect to CFC-11) is 0.82 [*WMO,* 2011] and it has a 100-yr global warming potential of 1,400 [*WMO*, 2011]. In 1987, Article 2 of the Montreal Protocol (MP) included regulations of CCl_4 under Annex B Group 2. CCl_4 production and consumption were eliminated for developed countries in 1996 under the amendments to the MP. Developing countries (i.e., Article 5 countries) were allowed some phase down production and consumption until fully banned in 2010. CCl_4 continues to be legally used as a contained feedstock, e.g. for the production of hydrofluorocarbons (HFCs), since feedstock uses are not regulated by the Montreal Protocol.

The primary sinks for CCl_4 include photolysis loss in the stratosphere, degradation in the ocean and the soil [*SPARC,* 2013]. The current best estimate of total lifetime (τ) for CCl_4 is 25 years [*SPARC*, 2013], relatively unchanged from the *WMO* [2011] assessment (26 years). A best estimate of the atmospheric partial lifetime (τ_{atmos}) for CCl_4 is 44 years [*SPARC*, 2013]. The best estimates of partial lifetimes due to the ocean sink (τ_{ocean}) and the soil sink (τ_{soil}) are approximately 81 (71-167) years and 195 (108-907) years [*SPARC, 2013*], respectively.

The MP controls have led to declining CCl_4 levels in our atmosphere at a rate slightly greater than 1% per year [*WMO*, 2011]. Under the MP Article 7, each Party provides CCl_4 data to the Ozone Secretariat on production, imports, exports, feedstock amounts, and amounts destroyed. The current CCl_4 bottom-up emissions estimate from the MP parties based on reported

production and feedstock usage (bottom-up estimate) was zero after 2007 [*WMO*, 2011]. There are also no known substantial stocks of CCl_4 in existing equipment or storage containers; thus, a $\tau \sim 25$ years would imply an annual decrease of 4% per year rather than the observed 1%. The atmospheric CCl_4 observations and the current total lifetime can be used to derive a top-down estimate of global emissions. This top-down emission estimates for 2007 and the following years were upward of 50 Gg per yr (Gg/yr) [*WMO*, 2011]. This very large difference of emission estimates is equivalent to approximately ~1,600 railroad tank cars of liquid CCl_4 lost each year.

The difference between the top-down and bottom-up emission estimates suggests that there is an unreported source of CCl_4. Recent work by *Fraser et al.* [2013] suggests that emissions from contaminated soils, toxic waste treatment facilities, and possibly chloro-alkali plants could be contributing 10-30 Gg/yr. *De Blas et al.* [2011] also observed excess CCl_4 above the background in Bilbao, Spain (similar to the Fraser et al. observations near Melbourne, Australia), and attributed this to an unidentified source near the measurement site. *Odabasi* [2012] found that mixing of bleach with surfactants or soap could form CCl_4, but global emissions from this source have not been estimated. Emissions from CCl_4 feedstock uses are highly uncertain [*TEAP*, 2011], but have been estimated to be approximately 0.5% of the total feedstock used (equivalent to 5 Gg/yr for 2011 production) [*Miller and Batchelor*, 2012]. None of these potential sources alone can fully explain the 50 Gg/yr discrepancy between the top-down and bottom-up emission estimates.

In this paper, we use available source and sink data in global and box models to test the compatibility of the existing emission and lifetime estimates with CCl_4 mixing ratio observations. In particular, we present the most likely emission and lifetime scenarios that close the current gap and best reconcile the observed trend in concentrations and their difference between the

88 Northern hemisphere (NH) and Southern hemisphere (SH) (i.e., the inter-hemispheric gradient or
89 IHG).

90 **2. Models and Simulations**

91 ***Models.*** We pair a 3-Dimensional (3-D) Chemistry Climate Model (CCM) with 1-box and 2-
92 box models to examine the atmospheric budget of CCl_4. The ***global 1-box model*** used in this
93 study is the same model used in recent WMO Ozone Assessments, and is described in detail in
94 *Velders and Daniel* [2013]. The global 1-box model has been used to derive top-down emission
95 estimates for long-lived ODSs using best-estimate lifetimes and observed surface mixing ratios
96 as constraints. The ***2-box hemispheric model*** is developed from the global 1-box model and
97 simulates both the long-term global trend and Northern-Southern hemispheric differences in
98 atmospheric concentrations of CCl_4. We assume ocean and soil losses in two hemispheres are
99 scaled exactly with ocean and soil area. The IHG is generated by the asymmetry in hemispheric
100 emission fraction and the ocean and land surface fractions in the two hemispheres. The 3-D
101 CCM used here is the NASA GEOS Chemistry Climate Model (***GEOSCCM***) Version 2, which
102 couples the GEOS-5 GCM [*Reinecker et al.*, 2008] with a detailed stratospheric chemistry
103 module [*Douglass and Kawa*, 1999]. A comprehensive evaluation of several CCMs over the
104 1960-2005 period shows that the GEOSCCM agrees well with observations for many of the
105 meteorological, transport-related, and chemical diagnostics [*Eyring et al.*, 2006]. Of particular
106 relevance to this study, GEOSCCM represents well the mean atmospheric circulation as
107 demonstrated by its realistic age-of-air, and further, realistic loss and atmospheric lifetimes for
108 long-lived ODSs [*Waugh et al.*, 2007; *Douglass et al.*, 2008; *Chipperfield et al*., 2014]. The
109 model also features realistic inter-hemispheric transport and reproduces well the observed IHG in

previous flux-based simulations of major long-lived ODSs [*Liang et al*., 2008; *Chipperfield et al.*, 2014]. A detailed description of the box models and the GEOSCCM is in Appendix A.

While the 3-D GEOSCCM is used to understand how various processes impact CCl_4 concentrations in a more realistic modeled atmosphere, the box models provide top-down emissions and lifetime estimates that are consistent with the observed surface mixing ratios. Pairing the simple box models with the 3-D GEOSCCM greatly enhances the computational efficiency of choosing emissions and corresponding lifetimes for the 3-D model simulations. The box models also provide useful conceptual tools to examine the sensitivities of CCl_4 mixing ratio observations to sources, sinks, and the atmospheric inter-hemispheric distributions of these quantities (2-box hemispheric model).

3-D Simulations. The global emissions in the 3-D simulations are top-down emission estimates consistent with the observed atmospheric CCl_4 decline when using the global 1-box model. CCl_4 is run with flux boundary conditions, using geographically resolved surface emissions originally described in *Xiao et al.* [2010]. Five simulations are performed (Table 1). The baseline run, Run A, is a 53-yr simulation with the SPARC 2013 photochemistry, soil and ocean lifetime recommendations, and the corresponding top-down emission derived using the global 1-box model. To better understand the factors that influence the CCl_4 budget, we conduct four additional model simulations (1995-2012), Runs B-E, with varying lifetimes, global emission and emission distributions. Runs B-E are initialized with the January 1995 Run A initial conditions.

3. Results

3.1 Discrepancy between bottom-up and top-down emissions estimates

We use the long-term surface observations of CCl_4 made by the National Oceanic and Atmospheric Administration – Global Monitoring Division (NOAA-GMD) [*Montzka et al.*, 1999; *Thompson et al.*, 2004] to derive the top-down emission estimates in the global 1-box model. The GMD dataset is a combination of in situ and flask samples, all based on Gas Chromatography – Electron Capter Detector (GC-ECD) analysis [Hall et al., 2011]. The global mean atmospheric CCl_4 is decreasing at a mean rate ~ −1.1 ppt per year since 1995 (Figure 1A). With a $\tau \sim 25$ years, this suggests a slow decrease in emission from ~ 80 Gg/yr from the late 1990s' to ~ 55 Gg/yr in the early 2010s' (Figure 1C). Reported industrial production and feedstock usage of CCl_4 suggests a rather sharp decrease in CCl_4 emissions from 100 Gg/yr in 1999 to near-zero emissions after 2007 (Figure 1C) if all CCl_4 is emitted in the year in which it was produced, as is generally expected. Such a drastic emission reduction rate is inconsistent with the observed CCl_4 decline.

We use the deviation of CCl_4 surface mixing ratios from the linear decay line to estimate year-to-year changes in annual emissions. After removing the least-squares linear fit (2000-2012) from each NOAA GMD station, we apply a 25-month ½-amplitude Gaussian low-pass filter to the observations (Figure 1B). The filtering reveals 3 periods of change: 1) from 1995-2005 a continuous increase in CCl_4 anomalies across all stations (mean ~+0.2 ppt/yr) with an increase of 0.6 ppt from 2003 to 2005 (+0.3 ppt/yr), 2) from 2007-2011 a decrease of about 1 ppt (−0.25 ppt/yr), and 3) an anomalous jump of ~0.6 ppt beginning in about 2012 (+0.6 ppt/yr). Based on the global 1-box model estimate, a 1 ppt change in atmospheric mean CCl_4 is equivalent to ~ 25 Gg/yr change in emissions. Thus, these observed anomalies imply: 1) ~ +8 Gg/yr anomaly emissions in period 1 from 2003-2005, 2) a ~ −6 Gg/yr extra emission decrease between 2005-2008, and 3) an anomalous increase of +15 Gg/yr in 2012. These year-to-year changes in

observed CCl_4 anomalies are inconsistent with the bottom-up emissions estimate from reported production and consumption (Figure 1C).

These inconsistencies between the mean trend and year-to-year emission variations and the observed CCl_4 changes suggest that the bottom-up emissions estimate from reported production and consumption are likely incorrect.

3.2 The inter-hemispheric gradient

It has long been recognized that IHG is a qualitative indicator of emissions for long-lived chemical compounds [*Lovelock et al.,* 1973]. The results from our 3-D model simulations show a compact linear correlation between the model annual IHG and the annual global emissions for all individual runs (R = 0.92-0.98 for Runs A-D) (Figure 2a). Of course, changing the hemispheric emission ratio affects this ratio, as do changes to the distributions of loss between the hemispheres (see discussion below). The collective correlation coefficient between the two variables from all four runs is 0.96, despite the various emissions and lifetimes used in each model run. This implies that IHG can be used as an empirical proxy to quantitatively infer global emissions.

It is important to mention that model results suggest that the global mean IHG calculated using all grid points in each hemisphere is different than that calculated using only model values at the NOAA GMD stations, due to biased sampling using only station data (Appendix B). The model global mean IHG is ~1.2 ppt higher than the IHG calculated using the model grid point values sampled at the GMD stations. This difference remains rather constant between 1995-2012. As a result, we apply a +1.2 ppt correction factor to the IHG calculated using the NOAA GMD station observations (1.5 ± 0.3 ppt). This corrected IHG is referred to as the NOAA GMD-

177 inferred IHG (IHG_{GMD}) in the rest of the paper, which ranges between 2.3-3.0 between 1995-
178 2012.

179 **3.3 3-D model simulations: Budget constraints from trend and inter-hemispheric gradient**

180 We use the global trend and the IHG as two independent constraints in the 3-D GEOSCCM.
181 All model runs, except Run E, are designed to reproduce the observed CCl_4 global trend. The
182 model IHG is then compared with IHG_{GMD} to assess various emission and lifetime scenarios that
183 best reconcile the observed IHG.

184 There are many factors that contribute to the CCl_4 IHG, including global emissions,
185 hemisphere emission fractions (EF_{hemis}), and soil and ocean loss rates. Despite a large range of
186 emission strengths, total and partial lifetimes used, runs A-D yield very similar IHG-emission
187 regression slopes (0.049-0.058 ppt/Gg yr^{-1}) (Figure 2a). These regression lines also show similar
188 zero-emission intercept points at 0.59-0.64 ppt (Figure 2a), the likely IHG that can be explained
189 by ocean and soil losses alone.

190 Of the range of parameters explored in the 3-D simulations, global emission strength plays
191 the dominant role in determining the IHG. Baseline Run A employed the highest emissions and
192 yielded the highest IHG between 3-5 ppt for 1995-2012, ~ 50% higher than IHG_{GMD}. This
193 suggests that the mean ~ 64 Gg/yr emissions estimate in Run A is likely biased high. To test this
194 emission level, Run B was employed with the lowest mean emission considered of ~ 35 Gg/yr.
195 Run B had the smallest IHG between 2.3-3.0 ppt for 1995-2012, agreeing well with IHG_{GMD}.
196 This is not surprising as Run B was designed from the 2-box model with global emissions that
197 would reproduce the observed gradient, albeit a corresponding lifetime increase to ~ 36.5 years
198 was necessary to match the long-term trend. The two runs with intermediate emissions (mean ~
199 50 Gg/yr) produce intermediate IHGs (2.6-3.7 ppt for Run C and 2.8-4.0 ppt for Run D).

In addition to changes in global emissions, Run C is designed to explore the sensitivity of IHG to changes in EF_{hemis}. We change EF_{hemis} from the baseline 94%NH:6%SH used in Runs A and B to 88%NH:12%SH. Run C shows a slightly smaller IHG/emissions regression slope (0.049 ppt/Gg vs. 0.053 ppt/Gg in Run A). This implies, to match the observed gradient, higher global emissions are needed if one assumes a larger fraction of emission resides in the SH. The result of this magnitude of repartitioning emissions into the SH is a relatively small reduction of the IHG, in comparison to the global emission strength.

The oceanic loss also affects the IHG. Run D features a latitude dependent ocean loss with a faster degradation in the SH. Faster SH ocean loss rates lead to a slight increase in the IHG (=< 10%). Again, this ocean loss rate impact on the IHG is small, in comparison to the global emission strength.

Run E is a special run in which we used global emissions consistent with the observed IHG, but lifetimes were kept the same as in SPARC [2013]. The Run E CCl_4 decreased at ~ 2.2 ppt/yr, double the observed rate. This suggests that while an average global emission ~ 35 Gg/yr is in better accordance with the observed IHG and the bottom-up estimate, there is a large discrepancy between this estimate and the current best estimate τ of 25 years for closing the global CCl_4 budget.

3.4 What impacts the inter-hemispheric gradient? – Insights from the 2-box hemispheric model

The 2-box hemispheric model yields a similar a strong linear relationship between the IHG and global emission as the 3-D GEOSCCM. With the inter-hemispheric exchange timescale ($\tau_{interhemis}$) set at ~1.7 years, the regression slope of IHG vs. emissions from the 2-box hemispheric model reference calculation (0.05 ppt/Gg, Figure 3 red symbols) agrees well with

223 the 3-D model hemispheric mean IHG from runs using the same EF_{hemis} and partial lifetimes.
224 The zero-emission intercept from the 2-box model is, however, only ~0.1 ppt, much lower than
225 the ~0.6 ppt value from the 3-D model. This is likely due to missing atmospheric processes that
226 could impact the IHG, e.g. stratosphere-troposphere exchange differences between the NH and
227 SH, or a simplified constant $\tau_{interhemis}$. Nevertheless, the similar IHG/emissions relationship
228 between the 3-D global model and the 2-box hemispheric model makes it possible to employ the
229 2-box hemispheric model to explore the important factors that determines the IHG.
230 Mathematically, IHG can be approximated using the following equation:
231 $$IHG = a + b \times Emission \quad (1)$$
232 Where *a* (unit of ppt) is the zero-emission intercept point and b (unit of ppt/Gg yr^{-1}) is the
233 regression slope on the scatter diagram. The value of *a* is a function of τ_{ocean}, τ_{soil}, EF_{hemis}, and
234 likely STE as well in the 3-D model, and *b* is mainly decided by EF_{hemis}.
235 We vary EF_{hemis}, τ_{ocean}, τ_{soil}, and τ_{atmos} to illustrate how changes in each variable regulate the
236 IHG (Figure 3). All 2-box hemispheric model calculations shown here use consistent emissions
237 and lifetimes that reproduce the observed global CCl_4 trend between 1995-2012. While the top-
238 down emission estimates are fixed for any specified lifetime input, the IHG can vary
239 significantly with changing EF_{hemis} (Figure 3a). A 100% NH emission (b = 0.066 ppt/Gg yr^{-1})
240 requires ~ 30-40 Gg/yr global CCl_4 emissions to reproduce the IHG_{GMD}. Decreasing the NH
241 release fraction greatly increases the total emissions necessary to capture the IHG_{GMD} (e.g,
242 b=0.026 ppt/Gg yr^{-1} for 70% release fraction in the NH, which requires emissions >75-115
243 Gg/yr). This 70% scenario is unlikely as the needed emissions greatly exceed the bottom-up
244 estimate - approaching the peak emissions ~ 120 Gg/yr in the 1970s' and 1980s' before CCl_4 was
245 regulated by the MP.

Changing partial lifetimes also impacts the IHG. Increases of τ_{ocean} (i.e., less loss, see Fig. 3b) decreases the IHG by decreasing the hemispheric contrast in ocean surface losses, reflected in the value of *a* in Eq. (1). As τ_{ocean} increases from 80 years to 240 years, *a* decreases from 0.21 ppt to 0.05 ppt. Increases of τ_{soil} (Fig. 3c) increase the IHG, and *a* increases from 0.08 ppt to 0.22 ppt as τ_{soil} increases from 200 years to 1000 years. Changing τ_{atmos} has little impact on *a* (Fig. 3d). Overall, these impacts are small. However, increases in τ_{ocean}, τ_{soil}, and τ_{atmos} can affect the calculated IHG to a greater extent through increases in total lifetime and the implied necessary decreases in emissions to match the observed trend. Hence, the 2-box hemispheric model calculations, similar to the 3-D model results, indicate that global emissions and EF_{hemis} play a dominant role in controlling the IHG with partial lifetimes associated with ocean, soil, and atmospheric losses contributing only minor modifications.

3.5 The likely emissions and lifetime scenarios

The 2-box hemispheric model, even with the least number of necessary processes considered in the present form, contains more unknown variables (τ, global emissions, EF_{hemis}) than constraints (observed trend and IHG). Hence, it is inadequate to uniquely close the CCl_4 budget mystery. Alternatively, we use the least root mean square deviation (RMSD) approach with our current best understanding of emissions and loss processes to rule out the unlikely EF_{hemis} scenarios and, furthermore, to infer an optimal total lifetime and emission scenario for each likely EF_{hemis}, as illustrated in Figure 4.

The RMSD of the calculated IHG suggests that the NH fractional emission is unlikely to be less than 80%, as a 70% or 76% NH emission fraction would yield an optimal total lifetime of ~ 20 years. This not only implies a much larger gap in total emissions needed to reconcile with the current bottom-up emissions estimate, but also significant decreases in partial lifetimes, both of

which are difficult to accommodate. The RMSD approach suggests that the likely NH emission fraction is between 80%-100%. This range implies average emission ~ 30-50 Gg/yr for 1995-2012 and optimal τ ~ 25-36 years, equal or longer than the current best estimates. A smaller NH fractional emission release requires a corresponding scenario of more global emissions and shorter τ to match the observed gradient, e.g. emission ~ 50 Gg/yr and τ ~ 25 years for a 80% NH emission fraction.

Assuming 100% emissions reside in the NH (b=0.066 ppt/Gg yr^{-1}) and using a mean IHG_{GMD} ~ 2.7 ppt and *a* ~ 0.6 ppt from the 3-D model in Eq. (1), we are able to determine the minimum mean global emissions necessary to match the atmospheric CCl_4 observations is ~ 32 Gg/yr between 1995-2012 and ~ 29 Gg/yr for the 2010s'. However, this requires a lifetime of 36 years, much longer than the 25 years current estimate. In the 3-D model Run B, we tested this 36-year lifetime by increasing τ_{atmos} to ~ 62 years and τ_{ocean} to ~ 160 years and leaving τ_{soil} unchanged. An increase in Run B's τ_{atmos} from 47 years to 62 years requires a ~ 60% reduction in the CCl_4 photolysis rate which greatly exceeds the lab-measured 15-20% cross section uncertainty range [*Rontu Carlon et al., 2010; SPARC*, 2013]. When comparing Run B's CCl_4 with two limited balloon profiles, this leads to a model high-bias in the critical stratospheric photolysis loss region (10-70hPa) (Figure A3). Keeping τ_{atmos} unchanged, a τ ~ 36 years means the summed lifetime against ocean and soil losses is > 150 years, which requires increases of both τ_{ocean} and τ_{soil} to the upper limit of the current best estimates (167 years for τ_{ocean} and 907 years for τ_{soil}). The above points to a need of re-evaluation of the current best estimates of partial lifetimes to address the possibility of a longer τ.

4. Summary and discussions

291 CCl_4 was increasing in the atmosphere until the early 1990s and is now in decline [WMO,
292 2011]. This decline is a result of the regulations imposed by the Montreal Protocol. The decline
293 during the 1990-2006 period was caused by a decrease in emissions and removal from the
294 atmosphere via loss processes [*WMO*, 2011; *SPARC*, 2013].
295 The current CCl_4 downward trend should be primarily determined by the lifetime, because
296 bottom-up emissions after 2007 are estimated to be near zero. However, from 2007-2012, the e-
297 folding time-scale of the decrease in the CCl_4 observations is about 66 years. This slow
298 downward trend cannot be reconciled with our current best estimate of the ~ 25 years (implied
299 top-down emissions ~ 55 Gg/yr between 2007-2012) derived from comprehensive chemistry-
300 climate models and atmospheric, ocean, and soil observations [*SPARC,* 2013].
301 Comparisons of mixing ratio observations with year-to-year variations of bottom-up
302 emissions estimates cannot be understood either. Much larger year-to-year CCl_4 fluctuations are
303 expected from the current time-series of bottom-up emissions estimate than are actually observed
304 in the atmospheric abundances. For example, between 1996 and 1998 the estimate of CCl_4
305 emissions jumped by about 80 Gg. Cumulatively, this 3-year period would have resulted in a 12
306 ppt increase in CCl_4 concentrations with respect to the slow decreases due to atmospheric, soil,
307 and ocean losses. Observations filtered to show these shorter time scale changes reveal
308 approximately a 1-2 ppt change of CCl_4. Such discrepancies indicate potential serious flaws with
309 CCl_4 emission reports.
310 Using a fully-coupled chemistry-climate model with a state-of-the-art photochemical loss
311 scheme for CCl_4, along with current estimates of CCl_4 oceanic and soil sinks, we have performed
312 a series of model simulations to constrain the atmospheric budget of CCl_4. The inter-hemispheric
313 gradient (IHG) of CCl_4 has been qualitatively used in the past to infer emissions of long-lived

ozone-depleting substances. Our CCM results suggest that the IHG provide useful information for *quantitatively* estimating CCl_4 emissions. We exploited the global trend and IHG as two independent constraints in this study to evaluate possible explanations for the discrepancy between top-down and bottom-up emission estimates.

The near-zero emissions from the UNEP reported production and feedstock usage in the recent years cannot be reconciled with these model estimates. At a minimum, a present-day global emission of 30 Gg/yr is required to reproduce the observed CCl_4 trend and IHG. It is most likely that ~80%-100% of the total global emissions are released in the NH. The likely range of global emissions and total lifetime (τ) associated with the above range of NH emission fraction remains large, varying from global emission ~ 30 Gg/yr and τ ~ 36 years for a 100% NH emission fraction to global emission ~ 50 Gg/yr and τ ~ 25 years for a 80% NH emission fraction. In the majority cases, this implied τ needed to reconcile the observed trend and IHG, is longer than the current best estimate lifetime (25 years). This would necessitate longer atmospheric, ocean and/or soil partial lifetimes than the current best estimates. Our findings point to the need of a more accurate bottom-up emissions estimate and/or lifetime estimate to close the CCl_4 budget mystery. Alternatively, information on fractional emission estimate from the two hemispheres, which is not well quantified currently, can also help in narrowing the likely range of global emission and lifetime.

Acknowledgements. This research was supported by the NASA GSFC GEOSCCM Modeling Group funded by the NASA MAP program.

334

335 **References**

336 Chipperfield, M. P., et al. (2014), Multi-model estimates of atmospheric lifetimes of long-lived
337 Ozone-Depleting-Substances: Present and future, accepted, *J. Geophys. Res*.,
338 doi:10.1029/2013JD021097.

339 De Blas, M., M. Navazo, L. Alonso, N. Durana, and J. Iza (2011), Trichloroethylene,
340 tetrachloroethylene and carbon tetrachloride in an urban atmosphere: mixing ratios and
341 temporal patterns, *International Journal of Environmental Analytical Chemistry*, 93(2), 228-
342 244, doi:10.1080/03067319.2011.629346.

343 Douglass, A. R., R. Stolarski, C. Jackman, M. Gupta, P. Newman, J. Nielsen, E. Fleming (2008),
344 Relationship of loss, mean age of air and the distribution of CFCs to stratospheric circulation
345 and implications for atmospheric lifetimes, *J. Geophys. Res*., *113*(D14), D14309,
346 doi:10.1029/2007JD009575.

347 Douglass, A. R. and S. R. Kawa (1999), Contrast between 1992 and 1997 high-latitude spring
348 Halogen Occultation Experiment observations of lower stratospheric HCl, *J. Geophys. Res.,*
349 *104*(D15), 18739–18754, doi:10.1029/1999JD900281.

350 Eyring V., et al. (2006), Assessment of temperature, trace species, and ozone in chemistry-
351 climate model simulations of the recent past*, J. Geophys. Res., 111*(D22), D22308,
352 doi:10.1029/2006JD007327.

353 Fraser, P. J., et al. (2013), Australian carbon tetrachloride (CCl_4) emissions in a global context,
354 accepted, *Environ. Chem*.

355 Hall, B. D., G. S. Dutton, D. J. Mondeel, J. D. Nance, M. Rigby, J. H. Butler, F. L. Moore, D. F.
356 Hurst, and J. W. Elkins (2011), Improving measurements of SF6 for the study of

357 atmospheric transport and emissions, *Atmos. Meas. Tech., 4*, 2441-2451, doi:10.5194/amt-4-
358 2441-2011, 2011.
359 Liang, Q., R. S. Stolarski, A. R. Douglass, P. A. Newman, and J. E. Nielsen (2008), Evaluation
360 of emissions and transport of CFCs using surface observations and their seasonal cycles and
361 simulation of the GEOS CCM with emissions-based forcing, *J. Geophys. Res., 113*, D14302,
362 doi:10.1029/2007JD009617.
363 Lovelock, J. E., R. J. Maggs, and R. J. Wade (1973), Halogenated Hydrocarbons in and over the
364 Atlantic, *Nature, 241*, 194-196, doi:10.1038/241194a0.
365 Miller, M. and T. Batchelor (2012), Information paper on feedstock uses of ozone- depleting
366 substances, Touchdown Consulting: 72.
367 Montzka, S. A., J. H. Butler, J. W. Elkins, T.M. Thompson, A. D. Clarke, and L. T. Lock (1999),
368 Present and future trends in the atmospheric burden of ozone-depleting halogens, *Nature,*
369 *398*(6729), 690-694, doi:10.1038/19499.
370 Odabasi, M. (2012), Halogenated Volatile Organic Compounds from the Use of Chlorine-
371 Bleach-Containing Household products, *Enrivon. Sci. Technol., 2008*, 42, 1445-1451,
372 doi:10.1021/es702355u.
373 Prinn, R. G., et al. (2000), A history of chemically and radiatively important gases in air deduced
374 from ALE/GAGE/AGAGE, *J. Geophys. Res., 105(14)*, 17,751-17,792,
375 doi:10.1029/2000JD900141.
376 Reinecker, M. M., et al. (2008), The GEOS-5 Data Assimilation System-Documentation of
377 Versions 5.0.1, 5.1.0, and 5.2.0, *Tech. Rep. 104606 V27, NASA*, Greenbelt, MD.
378 Rontu Carlon, N., D. K. Papanastasiou, E. L. Fleming, C. H. Jackman, P. A. Newman, and J. B.
379 Burkholder (2010), UV absorption cross sections of nitrous oxide (N_2O) and carbon

tetrachloride (CCl_4) between 210 and 350 K and the atmospheric implications, *Atmos. Chem. Phys.*, *10*, 6137-6149, doi:10.5194/acp-10-6137-2010.

SPARC (2013), SPARC Report on the *Lifetimes of Stratospheric Ozone-Depleting Substances, Their Replacements, and Related Species*, M. Ko, P. Newman, S. Reimann, S. Strahan (Eds.), SPARC Report No. 6, WCRP-15/2013.

Thompson, T. M., et al. (2004), *Halocarbons and other atmospheric trace species, Summary Rep. 27 2002-2003*, edited by R. C. Schnell et al., pp. 115-135, Clim. Monit. Diagn. Lab., U.S. Dep. Of Commer., Boulder, Colo.

TEAP (2011), UNEP *Report of the Technology and Economic Assessment Panel (TEAP), Progress Report*, Volume 1, coordinated by Lambert Kuijpers and Meg Seki, Nairobi, Kenya, 2011.

UNEP (2011), UNEP *Report of the Chemicals Technical Options Committee: 2010 Assessment Report*, United Nations Environment Programme, Ozone Secretariat, P.O. Box 30552, Nairobi, Kenya. http://ozone.unep.org/Assessment_Panels/TEAP/Reports/CTOC/

Velders, G. J. M. and J. S. Daniel (2013). "Uncertainty analysis of projections of ozone-depleting substances: mixing ratios, EESC, ODPs, and GWPs." *Atmos. Chem. Phys. Discuss., 13*, 28017-28066.

Waugh, D. W., S. E. Strahan, and P. A. Newman (2007), Sensitivity of stratospheric inorganic chlorine to differences in transport, *Atmos. Chem. and Phys*., 7, 4935-4941, doi:10.5194/acp-7-4935-3007.

WMO (2011), World Meteorological Organization) Scientific Assessment of Ozone Depletion: 2010, Global Ozone Research and Monitoring Project-Report No. 52: 572 pp, Geneva, Switzerland.

Xiao, X., et al. (2010), Atmospheric three-dimensional inverse modeling of regional industrial emissions and global oceanic uptake of carbon tetrachloride, *Atmos. Chem. and Phys., 10*(21), 10421-10434, doi:105194/acp-10-10421-2010.

Table 1. A description of the five 3-D GEOSCCM CCl_4 simulations used in this work.

	Description	Simulation Period	Average emission 1995-2012 (Gg/yr)	Hemispheric emission fraction NH:SH	Lifetime τ (yr)	Partial lifetimes (yr)		
						τ_{atmos}	τ_{ocean}	τ_{soil}
Run A	Baseline simulation	1960-2012	64 [a]	94%:6%	25.8	47	80	200
Run B	Decreased ocean loss, Decreased atmospheric loss forced by reducing the photolysis rate	1995-2012	35 [b]	94%:6%	36.5 [c]	62 [c]	160 [c]	200
Run C	Repartitioning of emissions into the SH with reduced global emissions.	1995-2012	50 [e]	88%:12%	30.7 [d]	47	160 [d]	200
Run D	[f] As Run C, but with latitude-dependent ocean loss rates with faster degradation in the Southern Hemisphere.	1995-2012	50	88%:12%	29.5	47	135	200
Run E	Same lifetimes as in Run A and same emissions as in Run B. This simulation does not match the observed CCl_4 decline.	1995-2012	35	94%:6%	25.8	47	80	200

[a] The global 1-box model top-down emissions estimate for $\tau \sim 25.8$ years.

[b] IHG-based annual emissions calculated using the average of IHG_{GMD} (section 3.2) and the IHG from the Advanced Global Atmospheric Gases Experiment (AGAGE) network [*Prinn et al.,* 2000] (Appendix B).

[c] τ, τ_{atmos}, and τ_{ocean} are determined using the global 1-box model in the forward mode with the IHG-based emissions and the observed global trend.

[d] For Run C, τ_{ocean} is determined using the 2-box hemispheric model by matching the IHG_{GMD}.

[e] The global 1-box model top-down emissions estimate for $\tau \sim 30.7$ years.

[f] The latitude-dependent ocean loss rates used are 1/288 yr^{-1} for 45-90°N, 1/222 yr^{-1} for 0-45°N, 1/122 yr^{-1} for 0-45°S, 1/75 yr^{-1} for 45-90°S. The relative strength of latitude-dependent loss rates are provided by Shari Yvon-Lewis (personal communication) and then scaled to give an ocean partial lifetime of 135 yrs.

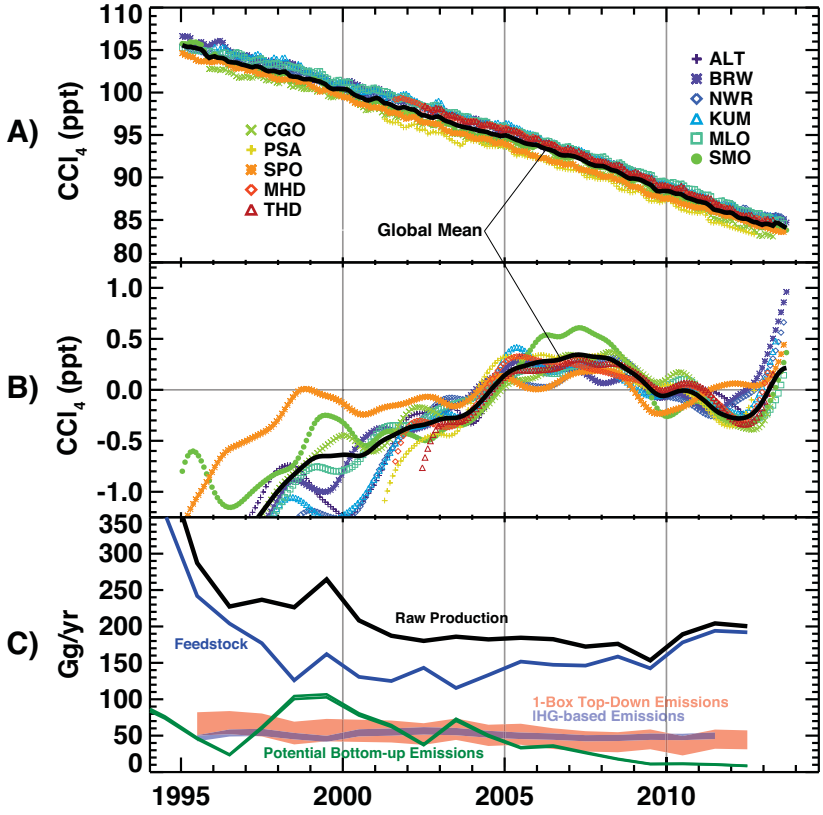

Figure 1. A) The observed CCl_4 mixing ratios at the NOAA GMD stations (color symbols) and the global mean values (solid black line). B) Same as A) but for mixing ratio anomalies. Note that some 2012-2013 data are preliminary, and have not yet undergone final calibration. C) CCl_4 emissions derived from atmospheric measurements (red and blue shading) and bottom-up potential emissions estimated from production data (green lines). The potential emissions estimate was derived from the difference between total CCl_4 production reported to UNEP (black line) and feedstock (line labeled). Red shading indicates the top-down emissions estimate from the global 1-box model using a total lifetime range of 25-36 yr. Blue shading indicates the IHG-scaled emissions using IHG_{GMD} and an empirically derived scaling factor with a range of 1/0.05-1/0.06 Gg yr^{-1}/ppt (section 3.5).

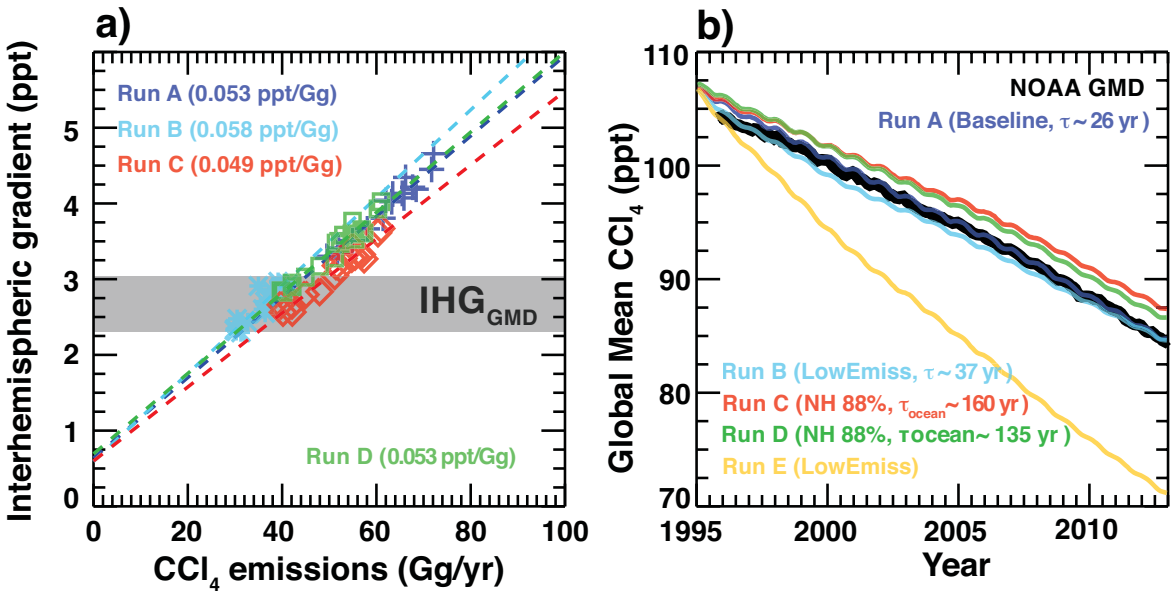

Figure 2. (a) The scatter diagram of model mean inter-hemispheric gradient vs. global annual emissions used in each model run between 1995-2012. Each symbol represents one annual-averaged value. The dashed lines (same color as the symbols) show the regression slope for each run. The gray shaded region indicates the IHG_{GMD} between 1995-2012. (b) The global mean CCl_4 mixing ratios from the NOAA GMD stations (thick black line) and model runs A-E.

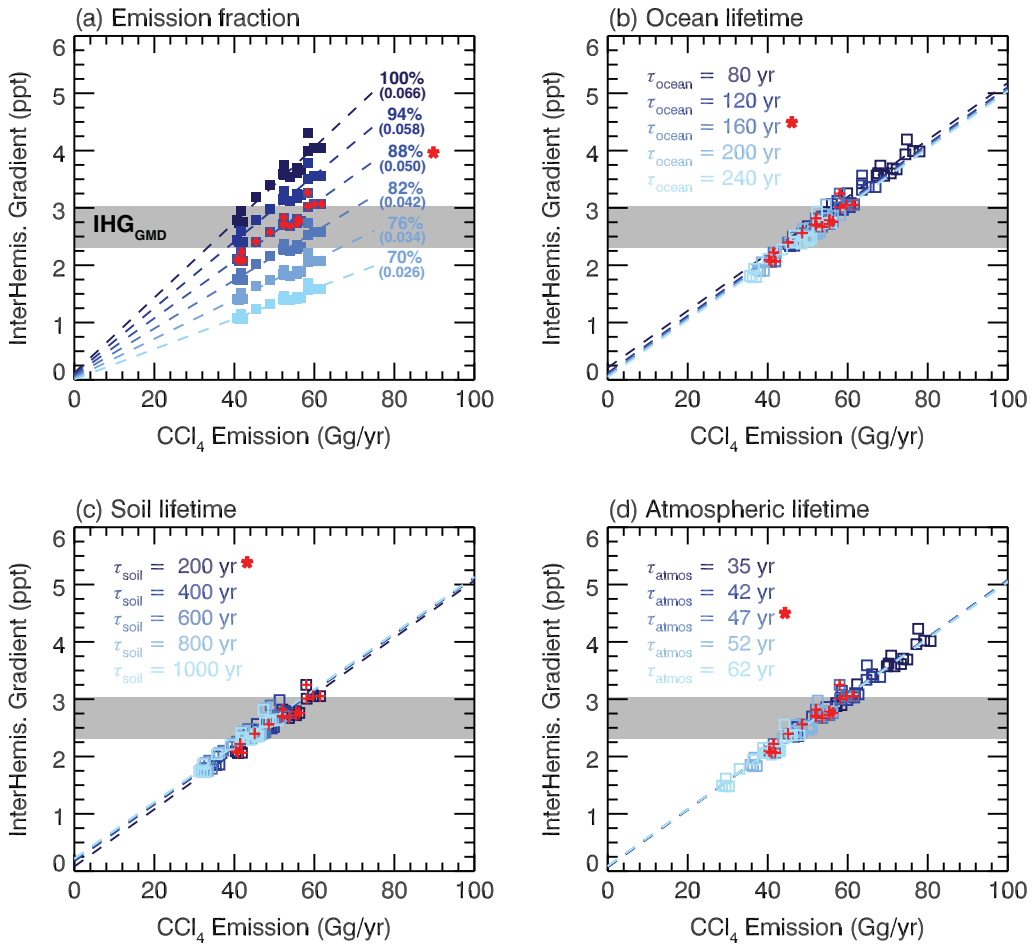

439

440 **Figure 3.** The red plus symbols on all panels show the scatter diagram of annual mean IHG vs.
441 global emissions between 1995-2012 from a reference calculation from the 2-box hemispheric
442 model. This reference calculation is equivalent to the 3-D model Run C, with a hemispheric
443 emission fraction of 88%NH:12%SH, τ_{ocean}=160 yrs, τ_{soil}=200 yrs, and τ_{atmos}=47 yrs. Each
444 symbol represents one annual-averaged value. The gray shaded region indicates the range of
445 IHG_{GMD} between 1995-2012. The groups of blue squares on each panel show the 2-box
446 hemispheric model sensitivity results by varying one of the input variables, (a) EF_{hemis} with
447 regression slope b (ppt/Gg yr^{-1}) shown in parenthesis, (b) τ_{ocean}, (c) τ_{soil}, and (d) τ_{atmos}, with
448 respect to the reference calculation. The dashed lines (same blue color as the symbols) show the
449 regression slope for each corresponding 2-box hemispheric model calculation.

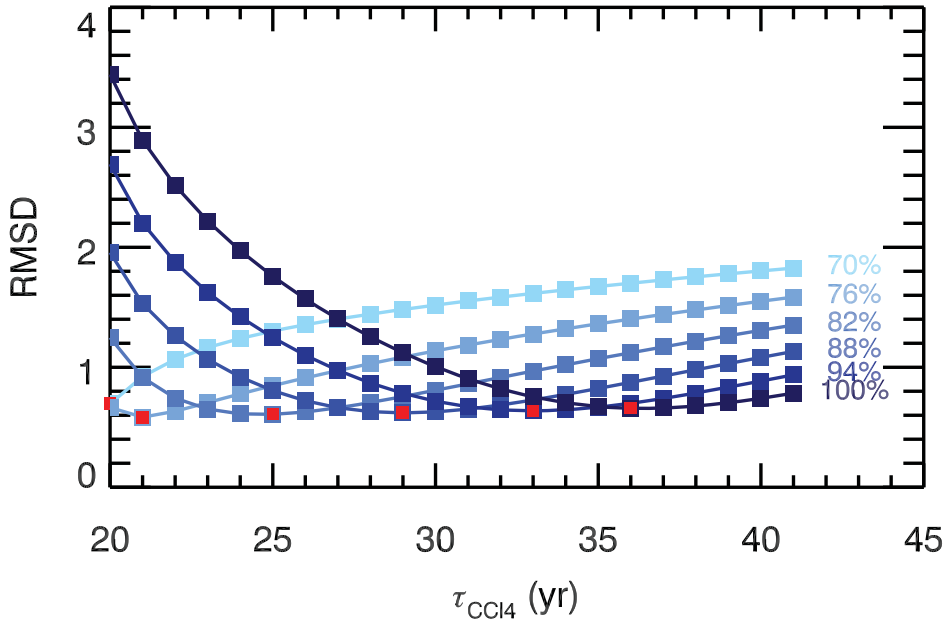

450

451 **Figure 4**. The root-mean-square-deviation (RMSD) of 2-box hemispheric model calculated IHG

452 (using the IHG_{GMD} as references) as a function of total lifetime for each assumed hemispheric

453 emission fraction (70%-100%). For each hemispheric emission fraction line, we highlight in red

454 symbols the optimal total lifetime that yields the least RMSD.